原子間力顕微鏡を用いたセンサータンパク Msb2p と Hkr1p の機械的性質測定系の構築

平本隆輔

東京大学大学院

新領域創成科学研究科

先端生命科学専攻

2011 年

修士論文

Construction of Mechanical Property Measurement System of Sensor Protein Msb2p and Hkr1p Using Atomic Force Microscopy

Ryusuke Hiramoto

Department of Integrated Biosciences
Graduate School of Frontier Sciences
University of Tokyo

2011

Master thesis

Table of contents

Acknowledgements

I would like to express my deepest gratitude to Professor Yoshikazu Ohya for his constant guidance and cheerful encouragement throughout this study.

I would like to my deep appreciation to Dr. Satoru Nogami for his consistent supervision and suggestion throughout my study.

I would like to thank collaborator Dr. Jürgen Heinisch and Dr Yves Dufrêne for their technical advises.

I would like to thank Dr. Takahiro Negishi, Dr. Shinsuke Ohnuki, Hiroki Okada and Tomohide Kobayashi for their helpful advice, discussion and encouragement.

I would like to thank all members of Laboratory of Signal Transduction, Department of Integrated Biosciences, Graduate School of Frontier Sciences, The University of Tokyo, for their warm encouragement.

At last but not least, I would like to thank my family for their financial support and for understanding of my study.

List of Figures

List of Tables

Abbreviations

AFM : atomic force microscopy

CRD : cystein rich domain

CWI : cell wall integrity

5-FOA : 5-fluoroorotic acid

HOG : high osmolarity glycerol

PCR : polymerase chain reaction

STR : serine-threonine rich region

ts : temperature sensitive

Abstract

In the yeast *Saccharomyces cerevisiae*, remodeling of cellular function is required for the response to extracellular stresses. This response is initiated when a sensor protein spanning the plasma membrane perceives stresses. However, its sensing mechanism towards variety of stresses is obscure. To obtain the details on the mechanism and function of a sensor protein, Dufrêne and his co-workers established a method to evaluate the mechanical properties of sensor proteins using the atomic force microscopy (AFM), and clarified that Wsc1p, a sensor protein of cell wall integrity pathway, behaves like a Hookean nanospring. It is possible that the Wsc1p perceives the tension of the glucan chain caused by stresses such as hypo-osmotic shock. The study further revealed that glycosylated Wsc1p perceives the mechanical tension enforced on the cell wall through its linkage with the glucan chain of the call wall. In hyperosmotic condition, cell wall is also subjected to change in its tension due to the rapid shift in turgor pressure. Thus, sensing mechanism of hyperosmotic environment is likely to have a similar property to Wsc1p, however, the difference and similarity of their sensing mechanisms were never investigated. Here I focused on Msb2p and Hkr1p, putative sensor proteins of high osmolarity glycerol (HOG) pathway which is activated by hyperosmotic shock, to clarify the nature of the sensor proteins and its sensing mechanism. In this study, I prepared the construct suitable for AFM analysis. The modified Msb2p was

confirmed its function and existence in mother cell surface. The construction and confirmation of the fusion protein is essential for the further study using AFM.

Introduction

Sensor proteins are essential for a detection of the stress exposure and an initiation of the appropriate latter stress response to adapt the extracellular stresses such as environmental alteration (Figure 1; Saier, 1994). In the budding yeast *Saccharomyces cerevisiae*, Msb2p and Hkr1p are putative sensor proteins to detect hyperosmotic stress and trigger to activate High Osmolarity Glycerol (HOG) pathway (Tatebayashi *et al.,* 2007; Wu *et al.,* 2006), where the HOG pathway is essential for acquiring a tolerance of external hyperosmotic condition (Figure 2; Hohmann, 2002).

In a high osmolarity environment, yeast cells synthesize glycerol to counterbalance the difference of intracellular and extracellular osmotic pressure. Because a malfunction of the hyperosmotic response system results in cell death under the fluctuating environments, the sensor proteins, Msb2p and Hkr1p, required for the system are crucial to survive (Tatebayashi *et al.,* 2007). In order to clarify the mechanisms of the system, both Msb2p (Multicopy Suppression of a Budding defect, Bender and Pringle, 1989) and Hkr1p (*Hansenula mrakii* Killer toxin-Resistant, Kasahara *et al.,* 1994) have been well studied, and many genetic studies indicated that Msb2p and Hkr1p are putative sensor proteins (Tatebayashi *et al.,* 2007: Wu *et al.,* 2006). However, their sensing mechanisms are still highly elusive because of lack of analysis method to examine the characteristic of sensor protein molecule *in vivo*.

Very recently, an innovative and elegant method using an atomic force microscopy (AFM) is developed, enabling us to obtain the mechanical properties of sensor protein molecule *in vivo* (Dupres *et al.,* 2009, Heinisch *et al.,* 2010a). The AFM is a very high-resolution type of scanning probe microscopy, with demonstrated resolution on the order of fractions of a nanometer. Dupres and his co-workers shed new light on the sensing mechanisms by using the AFM to measure a mechanical property of Wsc1p (for cell Wall integrity and Stress response Component, Verna *et al.,* 1997) which is a sensor protein in Cell Wall Integrity (CWI) pathway (Figure 2).

The CWI pathway is essential for cellular response against cell wall stress such as hypo-osmotic stress and heat stress (Levin 2005). When cells are exposed to these stresses, CWI pathway is activated, and eventually new cell wall is synthesized to acquire a tolerance for cell wall emergency (Heinisch *et al.,* 1999, Boorsma *et al.,* 2004). In this pathway, family of five putative sensor proteins are involved, namely Wsc1p, Wsc2p, Wsc3p, Mid2p and Mtl1p (Rajavel *et al.*, 1999, Verna *et al.*, 1997. Among them, Wsc1p is known as the most functionally major sensor protein to detect cell wall stress (Vay *et al.*, 2004).

In order to measure mechanical properties of Wsc1p, Dupres and his co-workers developed a modified Wsc1p, enabling us to contact Wsc1p with an AFM cantilever (Figure 3-A). By measurement of Wsc1p mechanical property with AFM, it is revealed that Wsc1p behaves like a Hookean nanospring.

Interestingly, in cells with cell wall stress exposure, spring constant of Wsc1p was reduced. It may indicate that Wsc1p spring property becomes sensitive to detect stress (Dupres *et al.,* 2009). It is also clarified that glycosylation of serine-threonine rich region (STR) of Wsc1p is essential for its nanospring property. Moreover, additional study estimates the possible functional model of Wsc1p. In this model, Wsc1p perceives the tension of the glucan chain, a cell wall component, alteration caused by cell wall stress contributed by anchoring of its cystein rich domain (CRD) to glucan chain (Ponting *et al.*, 1999). Wsc1p nanospring property functions as transmitter of tensile stress that causes conformational change in Wsc1p cytosolic domain whose active form is essential to trigger CWI pathway (Figure 3-B; Wilk *et al.*, 2010, Heinisch *et al.,* 2010b, Vay *et al.*, 2004). Thus the structural features of the sensor protein Wsc1p is strongly associated with the sensing mechanism of Wsc1p.

Two putative HOG pathway sensors, Msb2p and Hkr1p are structurally similar to Wsc1p. For example, they share two hydrophobic domains at the N-terminal end and in the C-terminal half, which could function as a signal peptide and transmembrane domain, respectively (Figure 4). Interestingly, Msb2p and Hkr1p also share O-glycosylation sites of STR (Kasahara *et al.,* 1994; Bender and Pringle, 1992), which is an essential domain in Wsc1p for Hookean nanospring properties contributed with glycosylation (Dupres *et al.,* 2009). Because, Msb2p and Hkr1p have similar structure to Wsc1p as shown in

Figure 4, I estimated that these two sensor proteins may also have specific mechanical property.

Although these three sensors share structural similarity, they detect opposite stress. Msb2p and Hkr1p detect hyperosomotic stress, whereas Wsc1p detects hypo-osmotic stress. Therefore I consider that comparison between the properties of Msb2p and Hkr1p to Wsc1p will provide us with a novel knowledge of general property as the functional sensor proteins and specific property for stress discrimination.

In this study, to understand sensing mechanism of HOG pathway sensor proteins Msb2 and Hkr1p, I prepared the constructs that are suitable for AFM measurement by modification of the sensor proteins. The modified Msb2p was confirmed its function by a suppression assay of the temperature-sensitive (ts) mutant *cdc24-4*, its existence in mother cell surface by immunostaining and tested for its exposure by nickel magnetic beads assay.

Results

Elongation of Msb2p and Hkr1p for AFM application

To investigate sensor protein properties *in vivo* by application of AFM, it is necessary that sensors are long enough to reach the cell surface. In the previous study of Wsc1p, the estimated length of extracellular part of Wsc1p is 87 nm considering from its number of amino acids in extracellular part (241 aa.) and length of peptide bond (0.36 nm, Dupres *et al.,* 2009). Because it is shorter than the average cell wall thickness (110 nm), addition of rod like STR of Mid2p, other putative CWI pathway sensor protein, on the N-terminal end of Wsc1p was essential to expose the Wsc1p to outside of cell wall. By the application of this calculation, I estimated Msb2p and Hkr1p lengths are 419 nm and 527 nm respectively. This estimation indicated that both proteins are long enough to reach the cell wall surface (Figure 4, 5). However, it is essential to compare the results of Wsc1p with that of Msb2p and Hkr1p, I decided to elongate Msb2p and Hkr1p by STR of Mid2p to equalize the measurement conditions.

Plasmid construction for expressing modified Msb2p and Hkr1p

Cloning of authentic MSB2 and HKR1 genes

To measure the protein property by AFM, insertion of an 8 x His-Tag is necessary for specific detection with AFM tips terminated with nickel nitrilotriacetate (NTA-Ni) groups (Figure 5). To synthesize modified Msb2p and

Hkr1p with 8 x His-Tag on the STR of Mid2p, I constructed three plasmids by following steps. Firstly, *MSB2* and *HKR1* genes with regions of promoter and terminator were amplified by high-fidelity PCR with primers (F-msb2apaI and R-msb2salI for *MSB2*, F-hkr1speI and R-hkr1sacI for *HKR1*, Table 3) with addition of restriction enzyme site at their tail from the Yeast genomic tiling collection vectors as templates (Open Biosystems, Catalogue# YSC4613). *Apa*I and *Sal*I sites for *MSB2*, and *Spe*I and *Sac*I sites for *HKR1* were added respectively. The resultant PCR products were inserted to vector pRS415 (pYO2633) of *Apa*I and *Sal*I sites for *MSB2*, and *Spe*I and *Sac*I sites for *HKR1* to yield pRS415MSB2 (pYO3061) and pRS415HKR1 (pYO3066) (Figure 6A). These plasmid sequences were read by cycle sequence with the primers (M13-20, msb2-1, msb2-2, msb2-3, msb2-4, msb2-5, msb2-6, msb2-7, msb2-8, msb2-9 and msb2-10 for *MSB2*, M13-20, hkr1-1, hkr1-2, hkr1-3, hkr1-4, hkr1-5, hkr1-6, hkr1-7, hkr1-8, hkr1-9, hkr1-10, hkr1-11, hkr1-12. hkr1-13 and hkr1-14 for *HKR1*, Table3) and confirmed not to possess mutation in *MSB2* and *HKR1* genes.

Insertion of URA3 maker gene

To use as negative selective marker for the substituting of *MID2* sequence in the latter process, *URA3* marker gene was integrated between regions of signal peptide and STR in both pRS415MSB2 (pYO3061) and pRS415HKR1 (pYO3066). The *URA3* sequence was amplified from the plasmid pRS316 using

primers (F-msb2ura, R-msb2ura, F-hkr1ura and R-hkr1ura) with the either *MSB2* or *HKR1* sequence of their tail for the homologous recombination, and co-transformed with either pRS415MSB2 (pYO3061) or pRS415HKR1 (pYO3066) into the yeast strain BY4741*Δmsb2* BY4741*Δhkr1* respectively for *in vivo* recombination. Transformants were selected on minimal medium without leucine and uracil (Figure 6B). The resulting plasmid containing a *URA3* marker inserted just prior to the STR (pYO3062 and pYO3067) was isolated and amplified in *E. coli* (Figure 6C).

Substitution of URA3 gene to STR of MID2 sequence

To substitute the *URA3* marker for the STR of Mid2p, the coding sequence for the *MID2* was amplified from Yeast genomic tiling collection (Open Biosystems, Catalogue# YSC4613) with the primers that codes for an 8 x His-Tag and the *MSB2* or*HKR1* sequence. Primers used for *MSB2* construct are F-mhismid2 and R-mhismid2, and primers used for *HKR1* construct are F-hhismid2 and R-hhismid2 (for sequence, see Table3). Each PCR product is co-transformed with the plasmids constructed above (containing *URA3*) into the yeast strains (BY4741*Δmsb2* and BY4741*Δhkr1*) for *in vivo* recombination and plated onto medium lacking leucine supplemented with 5-fluoroorotic acid (5-FOA) to select Leu^+ Ura^- cells (Figure 6D). Plasmid containing elongated sensor (pRS415MSB2-S/T-His; pYO3063 and pRS415HKR1-S/T-His; pYO3068) was recovered from the transformants (Figure 7-A, B).

Swapping of fusion Msb2 gene into overexpression vector

For adequate measurement with AFM, it is necessary that sample proteins localize in mother cell (Heinisch, personal communication), however it is observed that Msb2p specifically localizes to the bud neck and daughter cell (Tatebayashi *et al.,* 2007). For localization of fusion Msb2p in the mother cell, I sub-cloned the above fusion construct to a vector for overexpression. To make this plasmid, DNA fragment including fusion *MSB2* gene were digested with *Afl*II and *Sal*I and introduced in with the same restriction sites of pRS425 (pYO3011), 2-micron based multi copy vector, to yield pRS425MSB2-S/T-His (pYO3065) (Figure 7-C). Sequences of sensor genes in all acquired plasmids were confirmed by cycle sequence.

Functional confirmation of fusion Msb2p by suppression activity of temperature sensitivity of *cdc24-4*

To confirm whether the modified Msb2p functions like authentic Msb2p, the suppression ability of modified Msb2p was examined (Figure 8). Because *MSB2* was originally identified as a multi copy suppressor of the budding defect of *cdc24*-ts (Bender and Pringle, 1989), I transformed *cdc24-4* (YOC699) with pRS425MSB2-S/T-His (pYO3065) for the overexpression of fusion Msb2p (YOC4537), pRS425MSB2 (YOC4536) for the expression of authentic Msb2p and pRS425 (YOC4535) for negative control. Although *cdc24-4* (YOC699) grew

robustly at 32°C, grew very poorly at 34°C on YPD rich medium. *cdc24-4* with pRS425MSB2-S/T-His (YOC4537) grew at 34°C on YPD medium. Because original suppression activity of *MSB2* was observed in SD medium (Bender and Pringle, 1989), I repeated the same experiment on SD medium without leucine. Then, similarly weak suppression activity was observed (Figure 8). Although reproducible, the suppression results on agar plates were not obvious. Thus I further measured their growth phenotype with liquid YPD medium. Similarly to above, YOC4537, YOC4536 and YOC4535 were used in the experiment. Cells were grown at either at 32.5°C or 42°C in liquid YPD medium and the growth of the cells were recorded by measuring the OD660 of the culture. The growth among the strains were compared for their doubling time (Figure 9-A, B). Among each strains, no difference was detected for the doubling time, presumably due to the lack of sensitivity of the assay. This phenomenon of difference between solid and liquid culturing is often observed in yeast genetics. For instance, in this experiment using liquid YPD medium, not enough temperature sensitivity was observed at 34°C like the solid medium (Data not shown). The growth at 42°C was retarded compared to that of 32.5°C in the liquid culture.

Although these results indicate that suppression ability of *MSB2* is very weak, I concluded that the modified Msb2p is functional. I consider that fusion *MSB2* has weak suppression ability because there was a tendency of weak

suppression by repeated experiments using solid medium. To confirm more clearly, it is important to conduct other confirmation method such as the synthetic lethality rescued experiment.

Confirmation of overexpressed fusion Msb2p localizes in mother cell

To confirm whether overexpressed Msb2p localizes in mother cell, Msb2p localization was observed by immunofluorescent microscopy (Figure 10). First, I transformed BY4741 *Δmsb2* with pRS425MSB2-S/T-His (YOC4533). Then, to visualize the localization of modified Msb2p, I used His-Tag monoclonal antibody (Novagen) as a primary antibody after removal of cell wall with treatment of zymolyase (see Materials and Methods). After treatment with secondary antibody, cells were observed. The fluorescence signal was observed in whole cell, indicated that the fusion Msb2p localizes in mother cells by overexpression of fusion *MSB2* gene as I expected.

Confirmation of fusion Msb2p existence outside of cell surface

For the detection by AFM tip or the cantilever, it is essential that His-Tagged N-terminus of Msb2p must exist outside of the cell surface. To confirm this, anti His-Tag immunofluorescence was conducted with the cell without spheroplasting or having cell wall (see Materials and Methods). In this experiment, the fluorescence signal was observed in BY4741 *Δmsb2* with

pRS425MSB2-S/T-His (YOC4533) cell surface and not with vector control (Figure 11). This result indicates fusion Msb2p exist outside of cell wall, because cell wall prevents an invasion of antibody, fluorescence signal could not be detected if His-Tagged N-terminus of fusion Msb2p does not exist outside of cell. it also shows that the His-Tag conformation is accessible without spheroplasting. I tried further confirm this result, by treatment with nickel beads (Ni-NTA superflow) and showed the result in Figure 12. I expected that nickel beads bind the cells overexpressing fusion Msb2p. However, no significant difference of binding ability to nickel beads was observed between cells that overexpressed fusion Msb2p (YOC4533) and no Msb2p (YOC4532). Moreover, I performed similar experiment using Pure Proteome Nickel Magnetic Beads or nickel magnetic beads, but there was no significant difference (Data not shown). It is possible that the binding capability of beads is too weak to binding the cells, or number of the fusion proteins was insufficient to binding the cells. It is also possible that fusion Msb2p at bud neck is unable to contribute to bind the beads.

Although binding ability to nickel beads of cells that overexpressed fusion Msb2p was unremarkable, the result of immunofluorescence suggested His-Tagged N-terminus of fusion Msb2p exist outside of cell surface.

Discussion

In this study, in order to examine the mechanical properties of sensor proteins of HOG pathway, I produced the modified *MSB2* and *HKR1* constructs for AFM analysis. I confirmed sequence and function of the modified *MSB2* construct by using its ability to suppress temperature sensitivity of *cdc24-4*. Because suppression ability of *MSB2* was weak (Bender *et al.,* 1989), remarkable results could not be obtained from the growth assay using liquid medium. However, I consider fusion *MSB2* has weak or partial suppression ability because repeated agar plate experiments show tendency of suppression ability. In order for a sensor protein to be measured for its mechanical property using AFM, it is essential that the protein is expressed on the cell surface, especially in the mother cell, and the His Tagged-part of the protein is exposed to the cell surface beyond the cell wall because otherwise, the nickel nitrilotriacetate probe of AFM cannot access the protein. Thus I investigated whether the modified Msb2p existed at mother cell surface and the His-Tag is exposed at the cell surface using the methods of immunofluorescent microscopy and nickel magnetic beads assay. It was shown that, at least by overexpression, modified Msb2p localized in the mother cell and it was confirmed that the His-Tag is accessible at the cell surface as detection of the protein was possible without spheroplasting by immunofluorescent microscopy. To further confirm this result, I examined whether nickel beads or nickel magnetic beads bind the

cells with fusion Msb2p. However, there was no different of binding ability between the cells with fusion Msb2p and no Msb2p. It is possible that there are some problems about binding capability to cells. Although nickel beads assay failure to show binding ability of fusion Msb2p to nickel, result of immunofluorescence indicate that the construct is suitable for AFM analysis. Since I finished functional validation of the construct, I consider that the construct is now ready for AFM analysis with the collaborators, Dr. Heinisch and Dr Dufrêne. I will confirm the functions of modified Hkr1p, another sensor of HOG pathway, whether the synthetic lethality with deletion of *PTP2*, the tyrosine-specific phosphatase of Hog1p, is rescued by tetrad analysis. It is also important to confirm the localization and accessibility of Hkr1p also by immunofluorescent microscopy and nickel magnetic beads assay.

The modification of the proteins was performed for the sole purpose to be used for the measurement using AFM. As shown in Figure 4 and 5, the elongation by STR of Mid2p may not be necessary for the N-terminus of Msb2p and Hkr1p to be outside the cell wall, because adequate amino acids are thought to be located outside the plasma membrane. Addition of Mid2p-STR was conducted so that the result of AFM analysis is compatible to that of Wsc1p and it was shown previously that the elongation does not affect the function and mechanical property of Wsc1p (Dupres *et al.,* 2009). However, if the property of a sensor protein is the specific interest, it may be better to eliminate the

Mid2p-STR, and in fact, the construct is designed so that a single step recombination can achieve the elimination.

To test Msb2p and Hkr1p have mechanical properties that are functionally important in the response to the stress that activates HOG pathway, it is necessary that AFM analysis is performed under conditions hyperosmotic stress. One of the unique features of AFM is that the nano-scale measurement is possible *in vivo*. Thus cells under hyperosmotic stress such as sorbitol or NaCl treatment can be observed for the mechanical properties of the protein. Another unique feature of AFM is the measurement of affinity between the probe and the molecule in the order of pico-Newtons force sensitivity (Dupres *et al.,* 2009). Thus it is possible to draw a force-distance curve for each interaction detected, and as a result, Wsc1p was shown to have nanospring property which changes its spring constant when stress is applied (Dupres *et al.,* 2009). Through a similar analysis, it is expected that the modified sensor proteins of Msb2p and Hkr1p show the following behaviors by AFM analysis. Namely, the case which Msb2p and Hkr1p show mechanical behavior such as Hookean nanospring like in the case of Wsc1p, and the case which Msb2p and Hkr1p do not show the spring-like property. Considering the similarity in the secondary structure of the proteins, I expect the former case. In the former case, it is possible that Msb2p and Hkr1p perceive the tension of the glucan chain caused by stresses as well as Wsc1p. In this case, it is possible that Msb2p and

Hkr1p respond to the tension that opposite direction that Wsc1p does. In the latter case, it is possible that Msb2p and Hkr1p respond to other factors such as change in turgor pressure of plasma membrane.

It is suggested that STR of Msb2p and Hkr1p is highly glycosylated (Tatebayashi *et al.,* 2007), which support also that Msb2p and Hkr1p may have nanospring property, since glycosylation of STR of Wsc1p is essential for its Hookean nanospring property (Dupres *et al.* 2009). Analysis of glycosylation defective mutants of Msb2p and Hkr1p is also important to clarify contribution of STR domain to the property. It will be convincing to couple biological and biophysical approach to elucidate the function of the nanospring property. So far, it is known that deletion of the entire STR of Msb2p and Hkr1p constitutively induces reporter gene downstream of HOG pathway, even in the absence of any osmostress (Tatebayashi *et al.,* 2007). Therefore, it is suggested that the loss of nanospring property may alter the function of the proteins drastically.

Since Wsc1p is activated by hypo-osmotic stress, in the case of Msb2p and Hkr1p, which is activated by hyperosmotic stress, the response mechanism is thought to adverse to the mechanism of Wsc1p. However, the spring-like property maybe common to the both mechanisms, because it is a rapidly reversible property that can be considered advantageous in adapting frequently changing environment of the budding yeast. In addition, unlike the well-known sensor proteins of ligand-receptor type, mechanical sensors should be

advantageous because it is able to cope with variety of stresses because it senses the alteration in the pressure exerted on the cell wall, which can also explain why CWI and HOG pathways are activated in a number of different conditions (Levin, 2005, Hohmann, 2002). Study using AFM is expected to clarify the physical property which leads to the understanding of the coordination between the property and the functional mechanism to induce the down stream response against changes in cellular environment.

Materials and Methods

Media

The rich yeast medium (YPD) consisted of 1% Bacto yeast extract (DIFCO), 2% polypeptone (Wako), and 2% glucose (Nacalai Tesque). Yeast synthetic medium (SD) contained 0.67% Bacto yeast nitrogen base without amino acids (DIFCO), 2% glucose and appropriate nutritional supplements (Adnine sulfate, Uracil, L-Tryptophan, L-Histidine-HCl, L-Leucine and L-Lysine-HCl af the final concentration of 20 μg/ml, all supplements were purchased from Wako). Addition of 1 μg/ml 5-fluoroorotic acids (Toronto Research Chemicals) to SD produced FOA medium. *E.coli* LB medium contained 1% Trypton (DIFCO), 0.5% Bcto yeast extract and 1% NaCl (Sigma). Ampicililin (Meiji Seika) was added to the final concentration of 60 μg/ml to LB to produce LB+amp medium. For solid media, agar (Syouei Kanten) was added to the final concentration of 2 %.

Yeast strains, plasmids and oligonucleotides

The *Saccharomyces cerevisiae* strains used in this study are listed in Table 1. The plasmids and oligonucleotides (Synthesized by Greiner Japan) are catalogued in Table 2 and Table 3, respectively.

PCR

The *MSB2* gene fragment was PCR amplified with the primers with additional sequence for *Apa*I or *Sal*I site at their ends (F-msb2apaI and R-msb2salI Table 3) from Yeast genomic tiling collection (Open Biosystems, Catalogue # YSC4613). The *HKR1* gene fragment was PCR amplified with the primers with additional sequence for *Spe*I or *Sac*I site at their ends (F-hkr1speI and R-hkr1sacI for *HKR1*, Table 3) from Yeast genomic tiling collection. The PCR was conducted with KOD-plus polymerase (TOYOBO) using thermal cycler PTC200 (MJ Research). The PCR cycles are as follows; *MSB2* : 94°C for 15 sec, 65°C for 30 sec, 68°C for 5 min, 35 cycles and *HKR1* : 94°C for 15 sec, 57°C for 30 sec, 68°C for 6 min, 35 cycles. The *URA3* gene fragment was amplified with primers with additional sequence for *MSB2* or *HKR1* at their ends (F-msb2ura, R-msb2ura, F-hkr1ura and R-hkr1ura, Table 3) from plasmid pRS316 (Table 2). The PCR cycle is as follows (94°C for 15 sec, 48°C for 30 sec, 68°C for 1 min 20 sec) x 35 cycles. The STR of *MID2* gene was amplified with primers with additional sequence for part of sensor sequence for *MSB2* or *HKR1* and 8 x His-Tag (F-mhismid2 and R-mhismid2 for *MSB2*, F-hhismid2 and R-hhismid2 for *HKR1*, Table 3) from Yeast genomic tiling collection. The PCR cycle is as follows (94°C for 15 sec, 50°C for 30 sec, 68°C for 1 min) x 35 cycles.

Restrictive enzyme treatment

All restrictive enzymes were purchased from TAKARA Inc. unless noted.

The PCR amplified *MSB2* and pRS415 (Table 2) were digested with *Apa*I at 37°C for 3 hours in low-salt buffer followed by digestion with *Sal*I at 37°C for 3 hours in high-salt buffer. The PCR amplified *HKR1* and pRS415 were digested with *Spe*I at 37°C for 3 hours in low-salt buffer followed by digestion with *Sac*I at 37°C for 3 hours in high-salt buffer. The digested pRS415 (pYO2633) was treated with Calf Intestine Alkaline Phosphatase (TAKARA) followed by appropriate ligation reactions. To yield pRS425MSB2-S/T-His (pYO3065), pRS415MSB2-S/T-His (pYO3063) and pRS425 (pYO3011) were digested with *Afl*II and *Sal*I at the same condition.

Ligation, transformation, and plasmid preparation

Ligation was conducted with DNA Ligation Kit Ver.2.1 (TAKARA). Ratio of amount of substance of plasmid DNA and insert DNA was 1:2. Reaction was conducted at 16°C for 2 hours. This ligation sample was used for *E.coli* transformation using *E. coli* strain *SCS1* pretreated for chemical competent transformation, and was selected by LB + ampicillin medium. Bacterial transformation and pretreatment for chemical competence were conducted in the standard procedure (Inoue *et al*. 1990). Plasmids were prepared from liquid culture of *E. coli* harboring each plasmid using Quantum Prep Plasmid Mini Prep Kit (BioRad, #732-6100) accordingly to the manufacturer's protocol.

Yeast transformation

Cells were grown to a density of 1 x 10^7 cells/ml and washed with TE buffer (10 mM Tris-HCl and 1 mM EDTA pH8.0 (Sigma)). Cells were treated with 0.1 M lithium acetate (Nacalai Tesque) in TE for 1 hour and resuspended in 0.1 M lithium acetate containing 15 % glycerol (Wako) in TE. Cell suspensions were mixed with 50 % polyethylene glycol 4000 (Nacalai Tesque) in TE, heat shocked single stranded DNA and plasmid DNA. Volume ratio of cell suspension and polyethylene glycol solution was 3:7. After incubation for 1 hour at 25°C, cells were plated on selective medium and let grow for 3 – 4 days.

Plasmid isolation from yeast cells

Cells were grown for overnight in 1.5 ml selective medium. Collected cells were washed with 30 μl of STES buffer (0.5 M NaCl, 0.2 M Tris-HCl (pH 7.6), 0.01 M EDTA and 1 % SDS (Sigma)) and mixed. Collected washed cells were resuspended with 30 μl of same buffer and acid washed 0.4 mm glass beads (Sigma) were added. Mixed sample was vortexed for 5 min. This sample was added with 200 μl of TE buffer and 200 μl of 1:1 mixture of phenol saturated with TE (Nacalai Tesque) and chloroform (Wako), and vortexed for 2 min. This sample was centrifuged at 12,000 rpm for 5 min using a centrifuge M150-IVD (Sakuma). The aqueous phase was recovered. This aqueous phase was used for *E.coli* transformation after ethanol precipitation.

Cycle sequence

Cycle sequence was performed using BigDye Terminator v1.1 Cycle sequencing Kit (Applied Biosystems, #4337450). The PCR cycle is as follow (96°C for 10 sec, 50°C for 5 sec, 60°C for 4 min) x 25cycles. The primers used in cycle sequence are as follows and the specific sequences are listed in Table 3 (mid2-STR-last, M13-20, msb2-1, msb2-2, msb2-3, msb2-4, msb2-5, msb2-6, msb2-7, msb2-8, msb2-9 and msb2-10 for *MSB2*, mid2-STR-last, M13-20, hkr1-1, hkr1-2, hkr1-3, hkr1-4, hkr1-5, hkr1-6, hkr1-7, hkr1-8, hkr1-9, hkr1-10, hkr1-11, hkr1-12. hkr1-13 and hkr1-14 for *HKR1*, Table 3). After PCR reaction, ethanol precipitation was performed. These samples were resuspended with Hi-Di formamide (Applied Biosystems), and heat shocked (100°C for 2min). Electrophoresis for sequencing was done with ABI 3130XL according to the manufacturer's protocol (Applied Biosystems)

Suppression assay of ts strain *cdc24-4*

The strain *cdc24-4* (YOC699) was transformed with pRS425 (pYO3011), pRS425MSB2 (pYO3061), or pRS425MSB2-S/T-His (pYO3063). Transformants were grown on SD solid medium lacking leucine at 25°C, and colonies were restreaked on the same medium to obtain a single colony. To test complementation ability, the transformants and *cdc24-4* (YOC699) were plated

on YPD and SD lacking leucine plate, and incubated at 32, 32.5, 33, 33.5 and 34°C in water bath for 3 days.

Growth Assay

The strain *cdc24-4* (YOC699) was transformed with pRS425 (pYO3011), pRS425MSB2 (pYO3061), or pRS425MSB2-S/T-His (pYO3063) similarly to above. Transformatns were grown on SD liquid medium lacking leucine at 25°C and the log-phase culture was resuspended in YPD at the concentration of 1 x 10^6 cells/ml. The growth was monitored by measuring OD660 of the culture every 10 minutes at 32.5 or 42°C using Biophotorecorder (Advantec). This experiment was conducted with duplicate. Doubling time of these strains at each temperature was calculated from the growth data.

Immunofluorescence of fusion Msb2p

Cells were fixed using formaldehyde after grown to a density of 1 x 10^7 cells/ml. The fixed cells were washed with SP buffer (0.1 M KPi (pH 7.5, Wako) and 1 M sorbitol (Nacalai Tesque)) twice. To obtain spheroplasts, washed cells were treated with 2.8 unit/ml zymolyase 100T (Seikagaku Kogyo) and 0.2 % 2-mercaptoethanol (Nacalai Tesque) and incubated at 30 °C for 30 min. Cells were placed onto slide glass coated with poly-L-Lysine (Matsunami glass). In the case of cells with cell wall (without zymolyase treatment), cells were placed

onto slide glass coated with 0.1% Concanavalin A (Wako). His Tag monoclonal antibody (Novagen, #46-0693, Lot. 1265371) was used as a primary antibody against His-Tag (Tang *et al.,* 2008). This antibody was diluted 1:1000 with WT buffer (0.5 mg/ml BSA (Pierce), 150 mM NaCl, 50 mM HEPES (pH7.5, Nacalai Tesque), 0.1% Tween20 (Nacalai Tesque) and 1 mM NaN_3 (Wako)) and cells were treated with the antibody solution for 1 hour at room temperature. Then samples were washed with WT buffer four times. Secondary antibody, Alexa Fluor 488 conjugated anti-mouse IgG antibody (Molecular Probes), was diluted 1:100 with WT buffer. Cells were treated with secondary antibody solution for 1 hour at room temperature. Then samples were washed with WT buffer four times. After wash, the buffer was substituted with mounting buffer (1 mg/ml p-phenylenediamine (Sigma), 25 μM NaOH (Wako), 10% PBS (TAKARA) and 90% grycerol) and samples were covered with cover glass. Fluorescent microscopy were performed with Axiovision M3 (Carl Zeiss) using Axioimager with a x100 ECplan-Neofluar lens (Carl Zeiss) as an objective lens. Images were captured with CoolSNAP HQ cooled-CCD camera (Roper Scientific Photometrics) and Axio Vision software (Carl Zeiss).

Nickel beads assay

BY4741 *Δmsb2* was transformed with pRS425MSB2-S/T-His (YOC4533) or pRS425 (YOC4532). The cells with density of 1 x 10^7 cells/ml were treated

with same volume of nickel beads solution consisting Ni-NTA superflow (QIAGEN). These mixtures were incubated at 4°C with gently shaking overnight. The mixture was then let sink for a short while and the beads were mounted on slide glass for observation. These samples were observed and photographed by CoolSNAP HQ cooled-CCD camera (Roper Scientific Photometrics) and Axio Vision software (Carl Zeiss). Pure Proteome Nickel Magnetic Beads (Millipore) was also used.

Figures

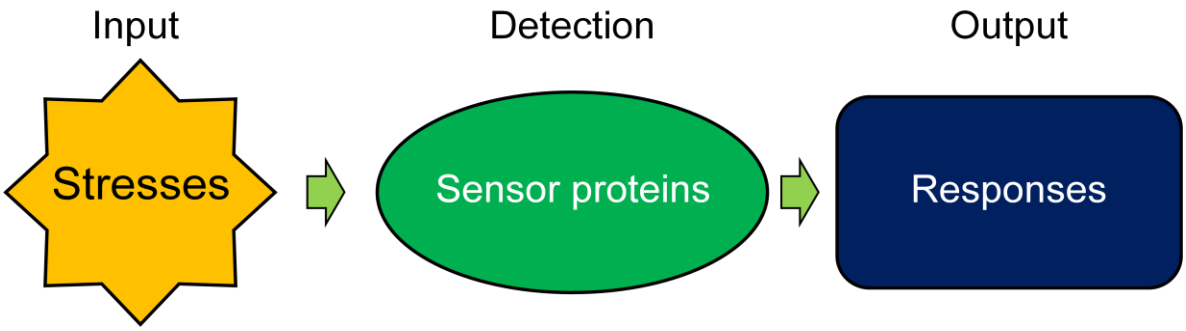

Figure 1. Sensor proteins are essential for respond to stresses.
Sensor protein is essential for stress detection and initiating latter cellular responses when cells are exposed with external stress such as environmental alteration.

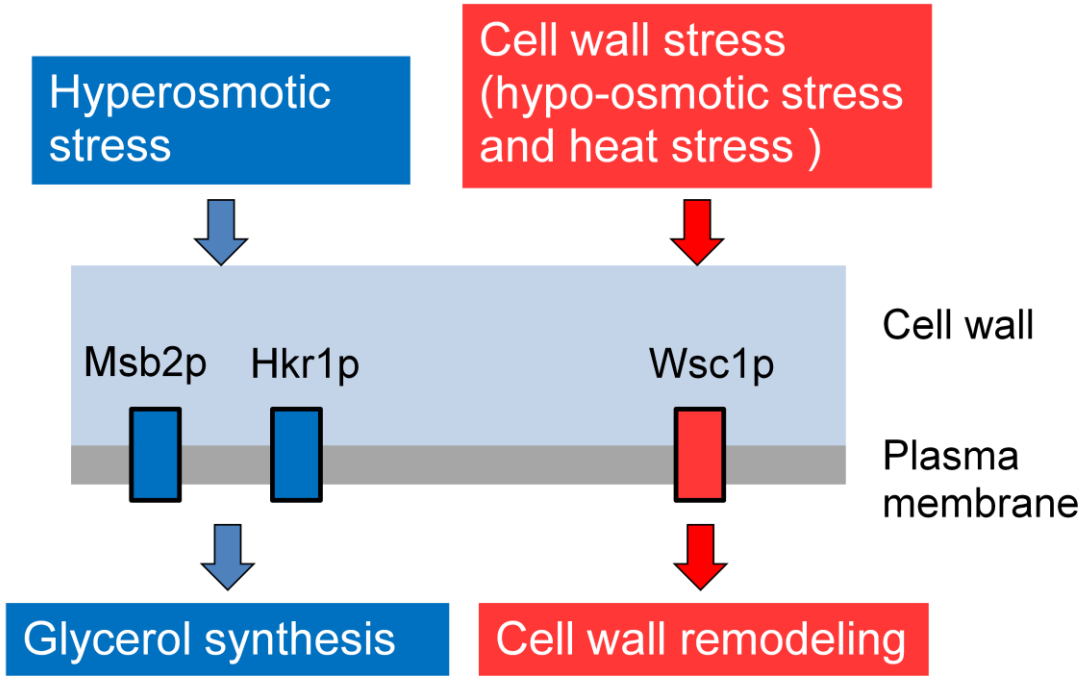

Figure 2. Two major pathways in response to extracellular stresses in yeast *Saccharomyces cerevisiae.*
Left: High osmorality glycerol (HOG) pathway which is activated by hyperosmotic stress. Msb2p and Hkr1p, the putative sensor proteins of HOG pathway, detect this stress and initiate cellular response to synthesizing glycerol for balancing the difference of intracellular and extracellular osmotic pressure.
Right: Cell wall integrity (CWI) pathway which is activated by hypo-osmotic and heat stress. Wsc1p, the putative sensor protein of CWI pathway, detects these stresses and initiate cellular response to synthesizing new cell wall for cell wall remodeling.

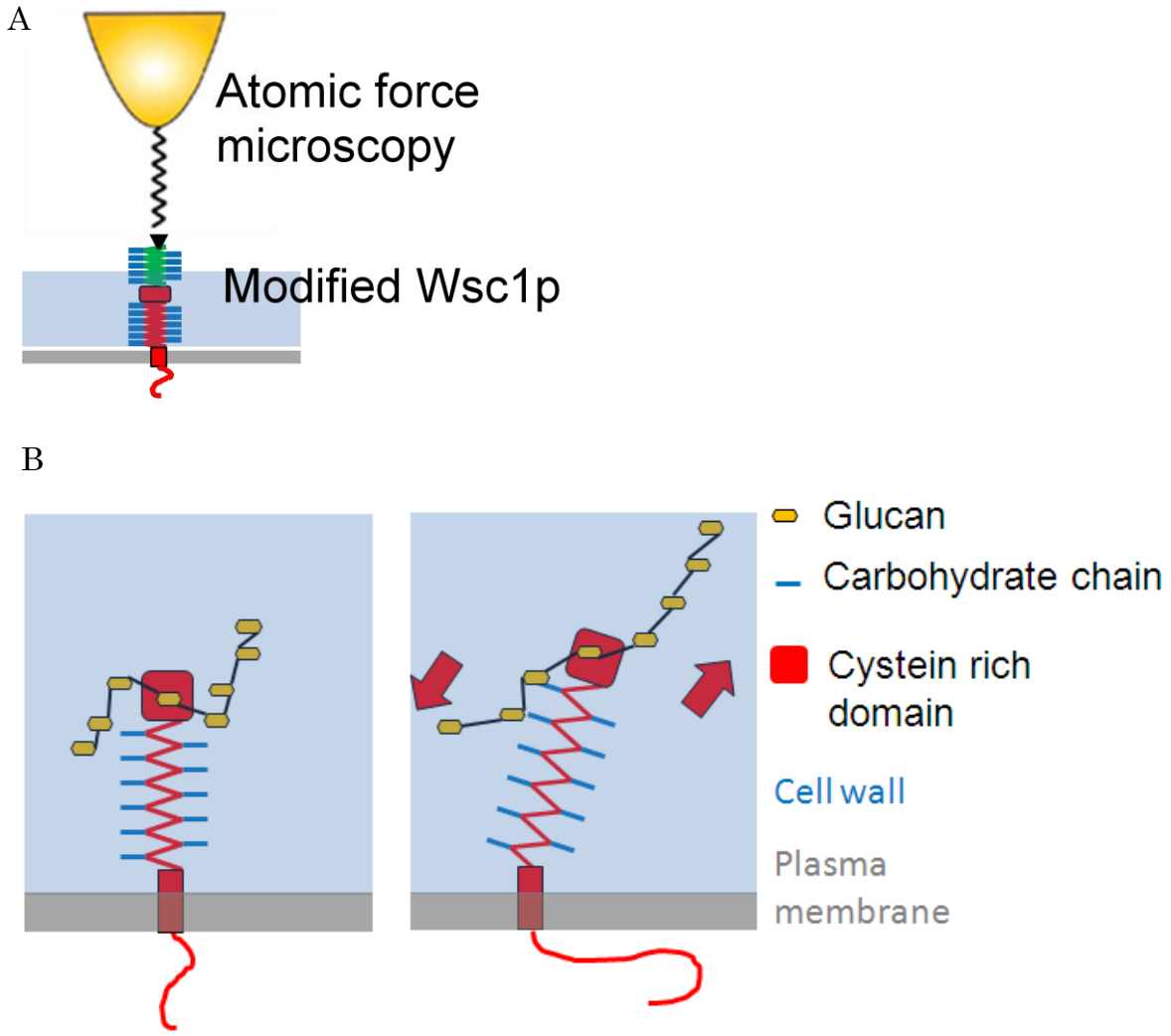

Figure 3. The schematic models of AFM analysis and sensing mechanism of Wsc1p (Heinisch *et al.*, 2010 modified).
(A) AFM analysis for sensor protein Wsc1p. The modified Wsc1p that enables binding to AFM cantilever is measured its mechanical property by pulling to upward using AFM. (B) Sensing mechanism of Wsc1p. Left side indicates no stress Wsc1p. The CRD of Wsc1p bind to glucan chain. Right side indicates Wsc1p under stress condition. The cell wall is changed by stresses and glucan chain receives the tension. Wsc1p senses this tension and undergo conformational change in its cytoplasmic domain. This conformational change triggers downstream signal transduction.

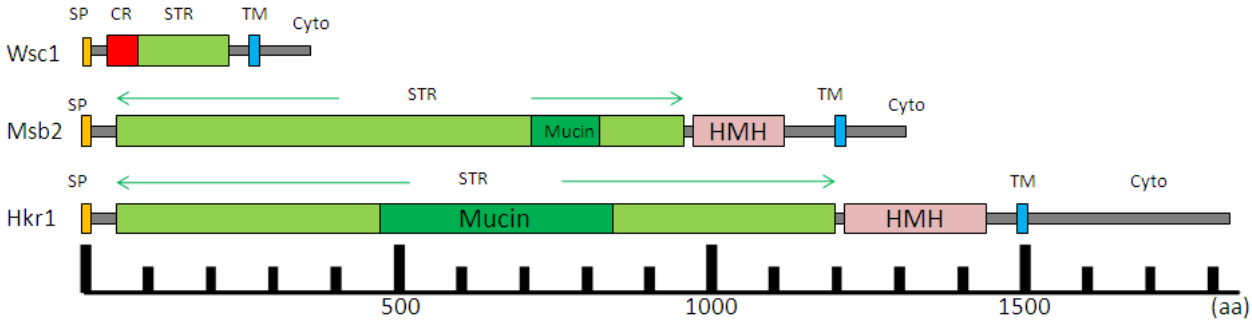

Figure 4. Schematic diagrams of the sensor proteins.
SP: Signal Peptide, CR: Cysteine-rich domain, STR: serine/threonine-rich domain, TM: Transmembrane domain, Cyto: cytoplasmic domain, Mucin: serine/threonine/prorine-rich mucin-like repeat, HMH: Hkr1-Msb2 Homology domain. STR of these three sensor proteins is highly glycosylated.

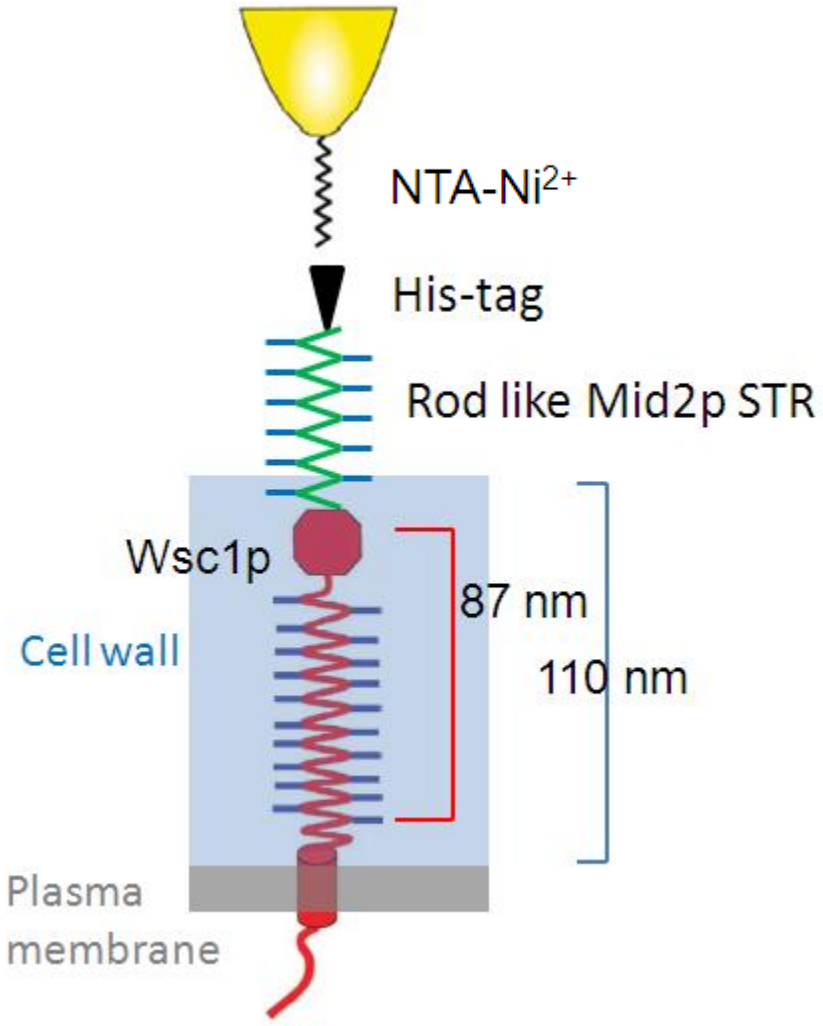

Figure 5. Modification of sensor proteins is essential for AFM analysis.
In case of Wsc1p, extracellular length is shorter than thickness of the cell wall. To reach the cell wall surface, Wsc1p is elongated with rod like protein, Mid2p. Moreover, to detect the sensor protein using NTA-Ni treated AFM cantilever, addition of the His-Tag is essential.

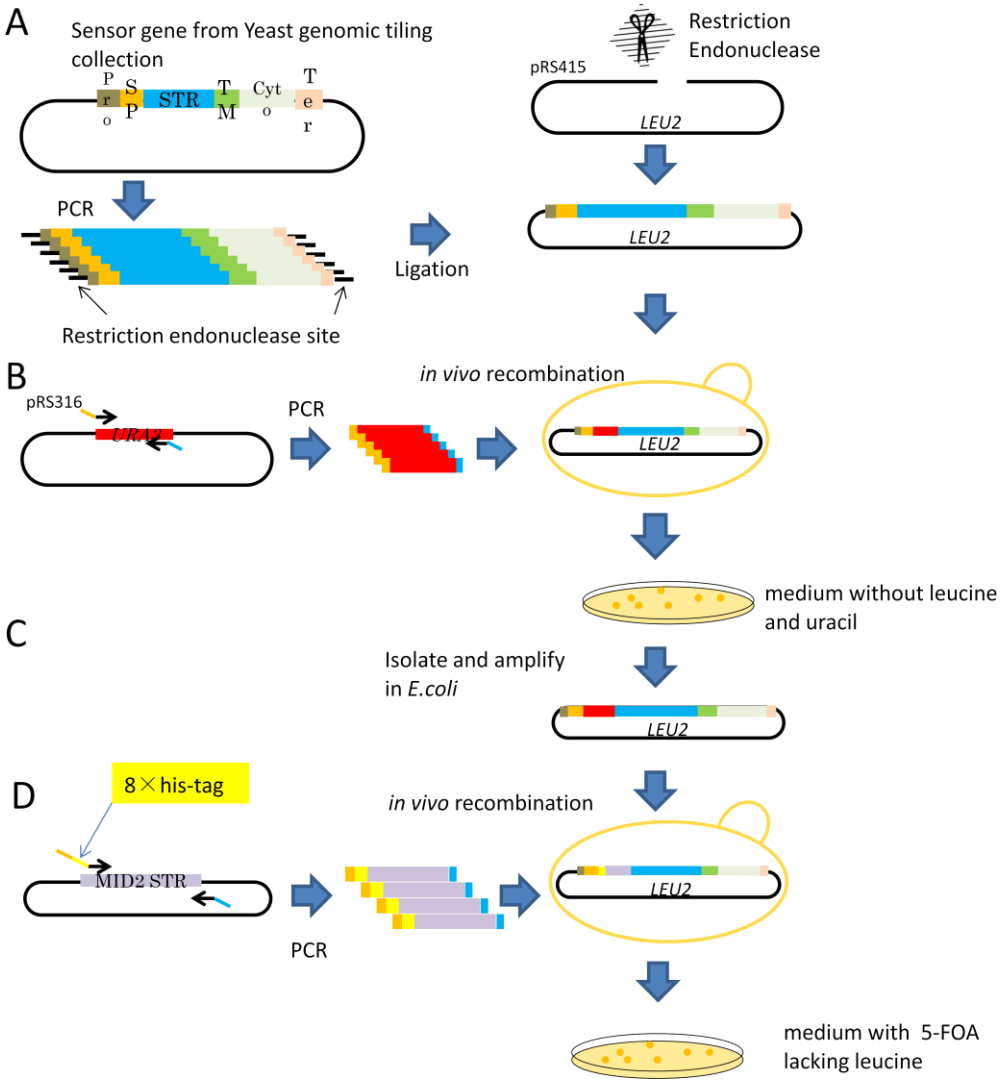

Figure 6. Schematic diagrams of modification of sensor for AFM measurement.
(A) The sensor gene is amplified by PCR. The PCR product is digested with restriction enzymes and cloned into the sites of the digested centromeric vector (pRS415). Pro is promoter sequence; SP is signal peptide; STR is serine-threonine rich domain; TM is Transmembrane domain; Cyto is cytoplasmic domain; Ter is terminator sequence. (B) The *URA3* gene is amplified from the pRS316. Two arrows mean primers. The orange part is a sequence of signal peptide of sensor gene; blue part is a sequence of STR of the sensor gene. The amplified *URA3* is co-transformed with plasmid containing sensor gene into the yeast strain for *in vivo* recombination. (C) Transformants are selected on minimal medium. The resulting plasmid is recovered from yeast and amplified in *E. coli*. (D) The *MID2* gene is amplified form a*MID2* containing plasmid using a forward primer with additional 8 x His-Tag. The PCR product is co-transformed with plasmid containing *URA3* into the yeast strain for *in vivo* recombination and plated onto medium lacking leucine supplemented with 5-FOA.

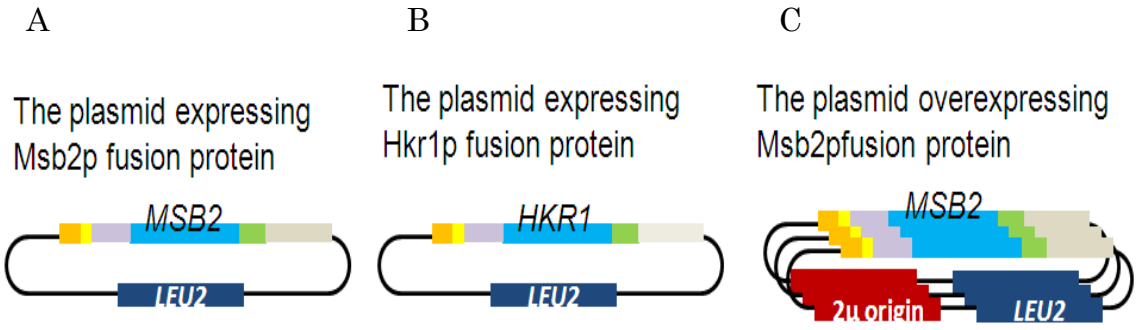

Figure 7. Three plasmids constructed in this study.
(A) pRS415MSB2-S/T-His (pYO3061): Plasmid for expression of Msb2p fusion protein. It is based on pRS415 vector and possesses *LEU2* marker. (B) pRS415HKR1-S/T-His (pYO3068): Plasmid for expression of Hkr1p fusion protein. It is based on pRS415 vector and possesses *LEU2* marker. (C) pRS425MSB2-S/T-His (pYO3063): Plasmid for overexpression of Msb2p fusion protein. It is based pRS425 vector and possesses *LEU2* marker and 2 μ origin.

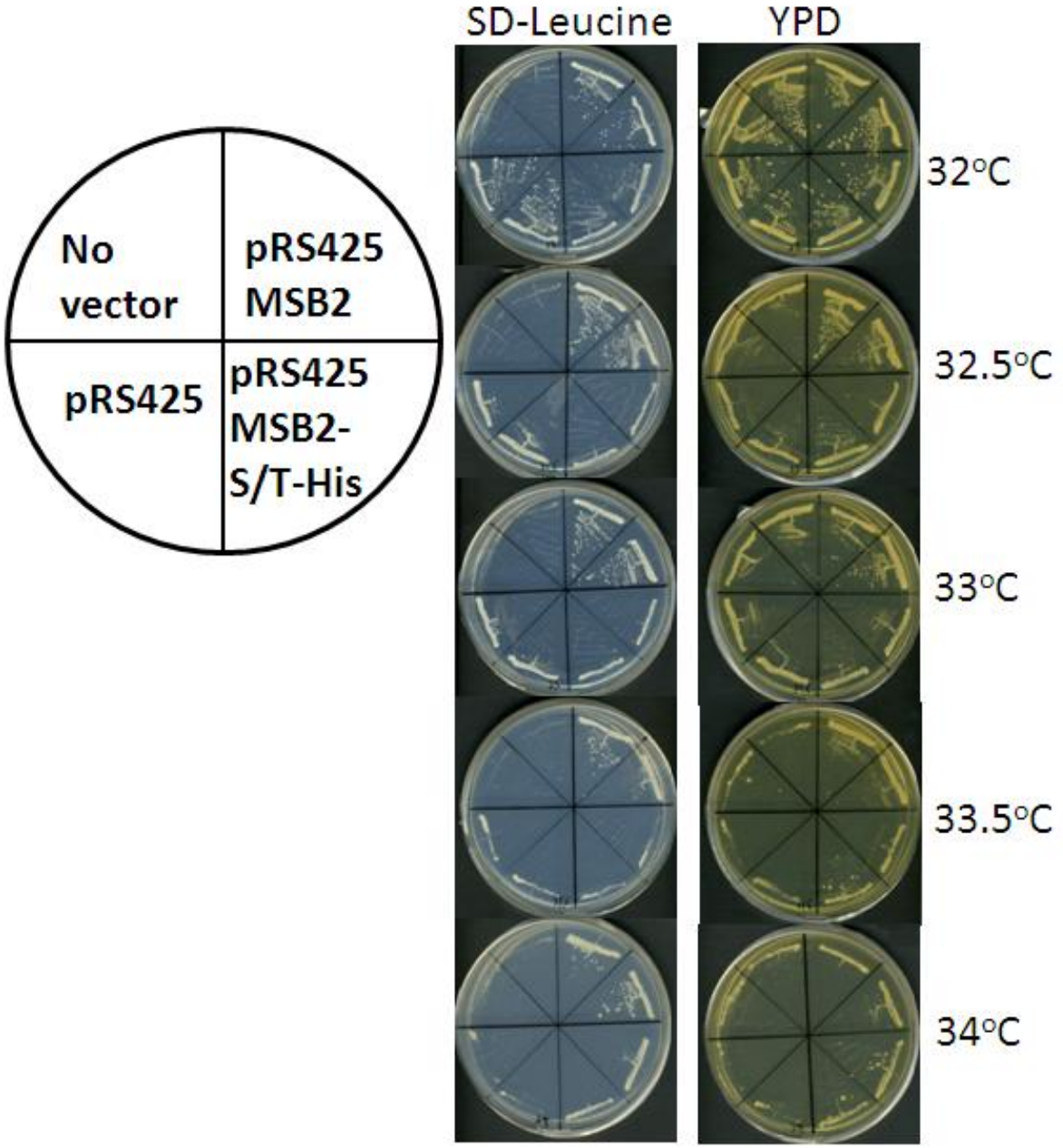

Figure 8. Suppression assay of ts strain *cdc24-4* (YOC699)
To test complementation ability, transformants and *cdc24-4* were streaked on YPD and SD lacking leucine plate, and incubated at 32, 32.5, 33, 33.5 and 34°C in water bath for 3 days.

A

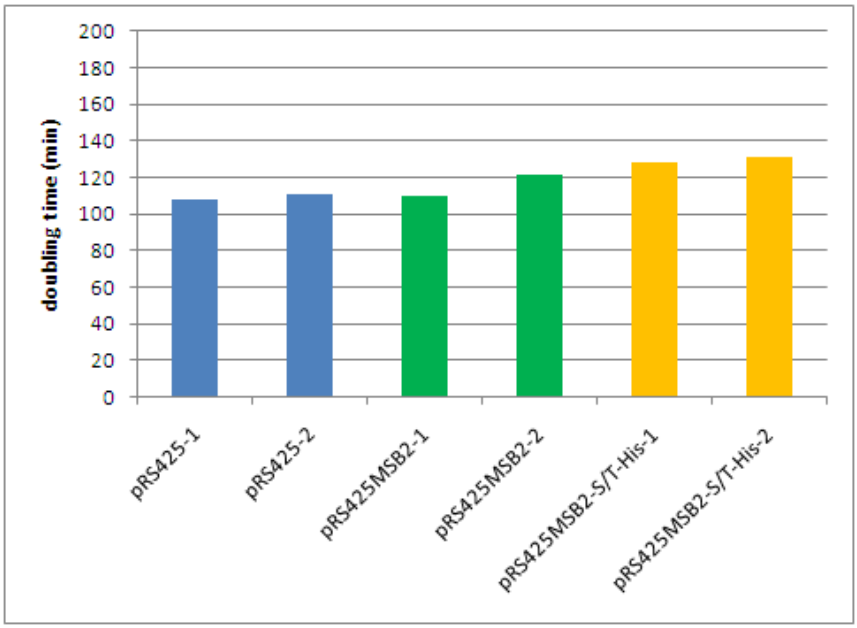

B

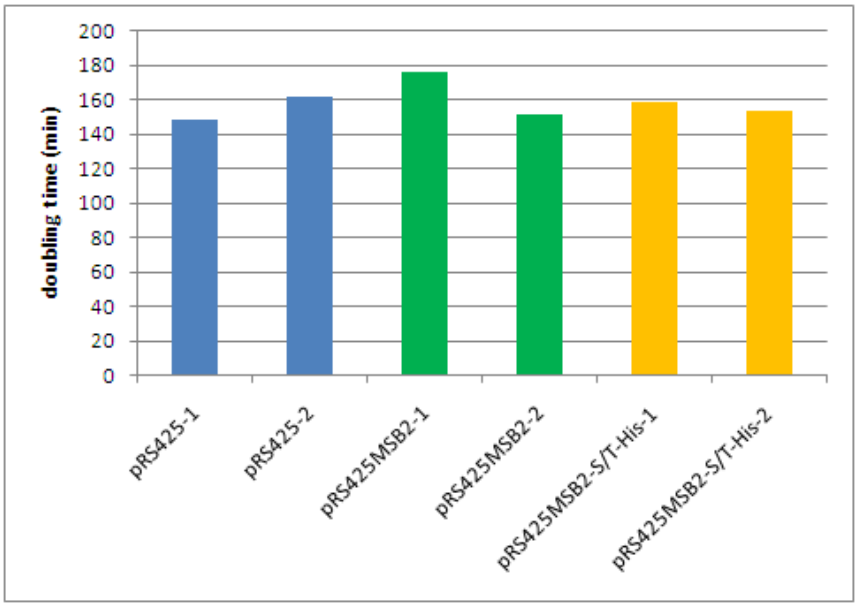

Figure 9. Doubling time of *cdc24-4* based transformants.
The strain *cdc24-4* (YOC699) was transformed with pRS425 (pYO3011), pRS425MSB2 (pYO3061), or pRS425MSB2-S/T-His (pYO3063). Transformatns were grown on SD liquid medium lacking leucine at 25°C and the log-phase culture was resuspended in YPD at the concentration of 1 x 10^6 cells/ml. The growth was monitored by measuring OD660 of the culture every 10 minutes at 32.5 or 42°C. Doubling time was calculated with these data. (A) Doubling time at 32.5°C, (B) Doubling time at 42°C are shown for transformants of indicated plasmid as duplicates (-1 and -2).

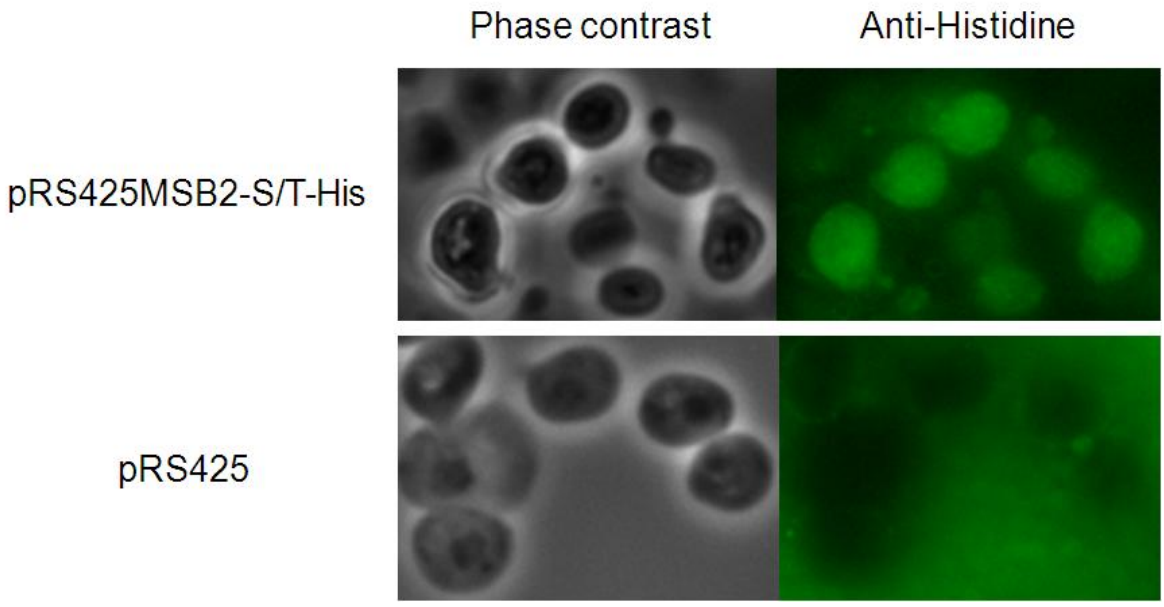

Figure 10. Overexpressed fusion Msb2p localizes in mother cells.
BY4741 *Δmsb2* was transformed with pRS425MSB2-S/T-His (YOC4533) or pRS425 (YOC4532). Cells at log phase were fixed treated with 1:1000 diluted His-Tag monoclonal antibody followed by treatment with 1:100 diluted Alexa Fluor 488 conjugated anti-mouse IgG antibody. Samples were observed using fluorescent microscopy.

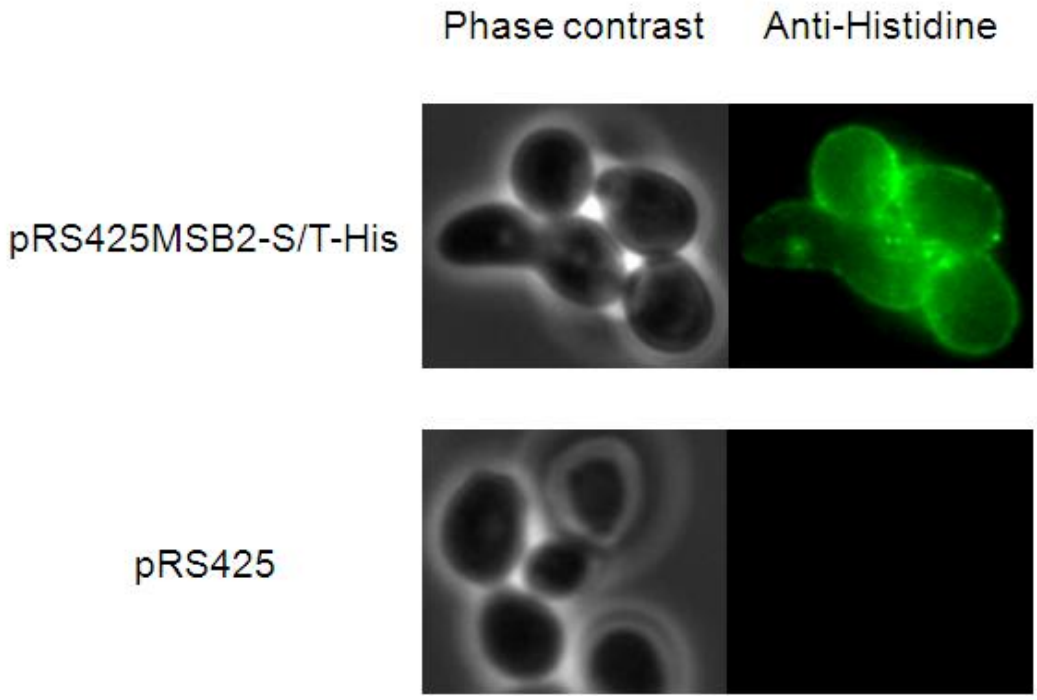

Figure 11. Overexpressed fusion Msb2p is surface-exposed.
BY4741 *Δmsb2* was transformed with pRS425MSB2-S/T-His (YOC 4533) or pRS425 (YOC4532). Cells with cell wall were treated with same antibody as used for the cells of Figure10.

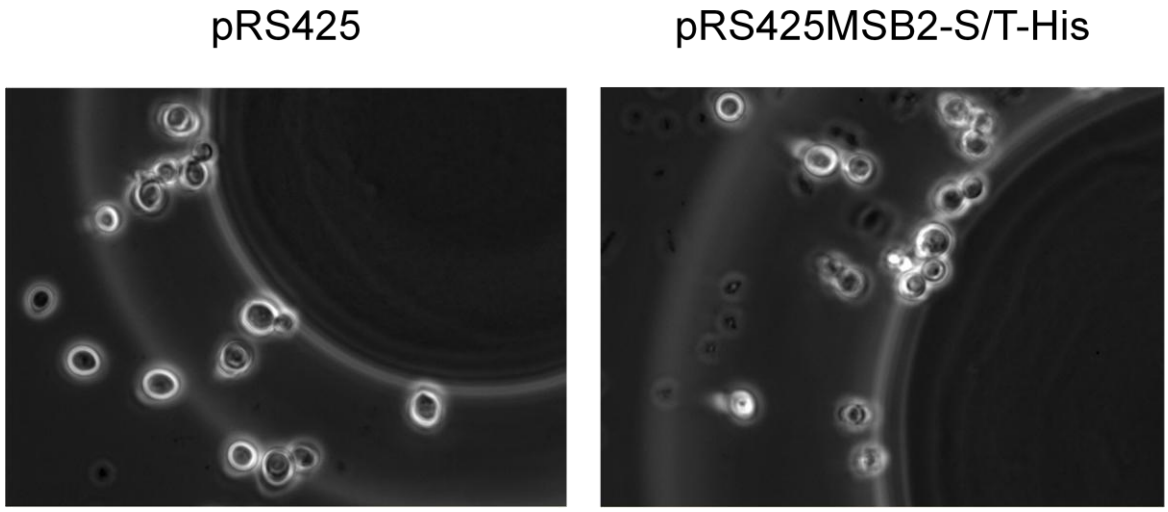

Figure 12. No significant difference of binding ability to nickel beads was observed between cells that overexpressed fusion Msb2p and no Msb2p.
BY4741 *Δmsb2* was transformed with pRS425MSB2-S/T-His (YOC4533) or pRS425 (YOC4532). These cells were treated with Ni-NTA and incubated for overnight at 4°C as described in Materials and Mehods. The large circular object on the right side of each photograph is the Ni NTA beads.

Tables

Table 1. Strains used in this study

Strain	Alias	Genotype	plasmid
YGR014W	BY4741*Δ msb2*	*Mat a; his3; leu2; met15; ura3; msb2::kanMX4*	
YDR420W	BY4741*Δ hkr1*	*Mat a; his3; leu2; met15; ura3; hkr1::kanMX4*	
YOC699	*cdc24-4*	*Mat a; his3; leu2; ura3; cdc24-4*	
YOC4532	BY4741*Δ msb2*-425	*Mat a; his3 leu2 met15 ura3 msb2::kanMX4*	pYO3011
YOC4533	BY4741*Δ msb2*-MSB2-S/T-Hi	*Mat a; his3 leu2 met15 ura3 msb2::kanMX4*	pYO3065
YOC4534	BY4741*Δ hkr1*-HKR1-S/T-His	*Mat a; his3 leu2 met15 ura3 hkr1::kanMX4*	pYO3068
YOC4535	*cdc24-4-425*	*Mat a; his3 leu2 ura3 cdc24-4*	pYO3011
YOC4536	*cdc24-4-MSB2*	*Mat a; his3 leu2 ura3 cdc24-4*	pYO3064
YOC4537	*cdc24-4-MSB2-S/T-His*	*Mat a; his3 leu2 ura3 cdc24-4*	pYO3065

Table 2. Plasmids used in this study

pYO No.	Name	Description
334	pRS316	used for *URA3* gene amplification
2633	pRS415	used for ligation, *Leu2* marker
3011	pRS425	2-m origin, *Leu2* marker
3061	pRS415MSB2	*MSB2*-inserted pRS415
3062	pRS415MSB2-URA3	*MSB2*-containing *URA3* sequence in pRS415
3063	pRS415MSB2-S/T-His	*MSB2*-containing 8 x His-Tag and STR of *MID2* in pRS415
3064	pRS425MSB2	*MSB2*-inserted pRS425
3065	pRS425MSB2-S/T-His	*MSB2*-containing 8 x His-Tag and STR of *MID2* in pRS425
3066	pRS415HKR1	*HKR1* inserted pRS415, *Leu2* marker
3067	pRS415HKR1-URA3	*HKR1*-containing the *URA3* sequence in pRS415
3068	pRS415HKR1-S/T-His	*HKR1*-containing 8 x His-Tag and STR of the *MID2* gene in pR

Table 3. Oligonucleotides used in this study

Name	sequence(5'–3')
F-msb2apaI	GCGCGGGCCCGAATTCCTCGGCGTCTACGAG
R-msb2salI	GCGCGTCGACGCATGCCGAACCTGTTGGATG
F-mhismid2	TTAGTGGGTCATTGGCCCGGGCCCACCATCACCACCATCACCATCATGCACGTTCTTCCGTAAGTAGAGT
R-mhismid2	GCGTTCCATTGCCGAATATAAAGTCGAAGGGGCTAGAAAGACCCGAACTTTTGGATT
F-msb2ura	TGTCTCCTATCGACCCTTGTAATTAGTGGGTCATTGGCCCGGGCCACCACGCTTTT
R-msb2ura	CTGAGCTTGTTGCGTTCCATTGCCGAATATAAAGTCGAAGGGGCTCGTTTACAATTT
msb2-1	CGACCTCACCAAGGGACCCC
msb2-2	GTTCATTCGCACCAGTCTGC
msb2-3	GGTGCCATTCCGGTGCAAAG
msb2-4	GTTGCTAGCTCCAGTACTGC
msb2-5	CAGGTGGCTCTAGCATGACC
msb2-6	ACCCTCTCAGACGACAACTC
msb2-7	AGCCCACCACTACATCCTCC
msb2-8	CATCCACTGCATCTTCTACC
msb2-9	AGTAACAGCAACTCTGGCGG
msb2-10	GGGTTGACAAATAATGACTC
F-hkr1speI	GCGCACTAGTCTGCAGTTGTCGTTATTTTTAATG
R-hkr1sacI	GCGCGAGCTCAAGCTTGGTAGGTTCTTCTC
F-hhismid2	CATTGTTAAATGCAATCGAGGCCCACCATCACCACCACCATCATGCACGTTCTTCCGTAAGTAGAGT
R-hhismid2	CATTATTGTATGAAGTTGAATATATTGTATCGTTACTATAAGAAAGACCCGAACTTTTGGATT
F-hkr1ura	AAAAAAATTTTACTCCTGGTGTCATTGTTAAATGCAATCGAGGCCACCACGCTTTTCAATTCAATTCATC
R-hkr1ura	TTCTATTCCATTATTGTATGAAGTTGAATATATTGTATCGTTACTATACGTTTACAATTTCCTGATGC
hkr1-1	AGTGTCCCTCGTAGGCACCTG
hkr1-2	AATGGCTGGCCAATATGGTG

Table 3. continued

hkr1-3	CTCCAGCATAACGGCAGCTTC
hkr1-4	TTCAGAGGCAAGTCAAGGTG
hkr1-5	CTGCCTATGCGTCTTCACCATC
hkr1-6	TCACCATCGGTACCTGTTGC
hkr1-7	CATCGGCTCTTGTTGTCCTG
hkr1-8	CCCTTCAGCTTCGAATTTGG
hkr1-9	CAAGCTTTACATCAACATTACG
hkr1-10	TCCCAATGCAATTGAACCGG
hkr1-11	AGCCGTAACATATCTTCAGC
hkr1-12	CTTTCCCGCTCTTCTTCTGG
hkr1-13	GGCACTGAATCATGTACTAC
hkr1-14	CACATAGGCTCACGCCATTAC
M13-20	GTAAAACGACGGCCAGT
mid2-STR-last	ATCCAAAAGTTCGGG

Reference

Bender A and Pringle JR. 1989. Multicopy suppression of the cdc24 budding defect in yeast by CDC42 and three newly identified genes including the ras-related gene RSR1. Proc Natl Acad Sci U S A. Dec;86(24):9976-80.

Bender A and Pringle JR. 1992. A Ser/Thr-rich multicopy suppressor of a cdc24 bud emergence defect. Yeast. Apr;8(4):315-23.

Boorsma A, de Nobel H, ter Riet B, Bargmann B, Brul S, Hellingwerf KJ, Klis FM. 2004. Characterization of the transcriptional response to cell wall stress in Saccharomyces cerevisiae. Yeast. Apr 15;21(5):413-27.

Dupres V, Alsteens D, Wilk S, Hansen B, Heinisch JJ, Dufrêne YF. 2009. The yeast Wsc1 cell surface sensor behaves like a nanospring in vivo. Nat Chem Biol. 5(11):857-62.

Heinisch JJ, Dupres V, Alsteens D, Dufrêne YF. 2010. Measurement of the mechanical behavior of yeast membrane sensors using single-molecule atomic force microscopy. Nat Protoc. 5(4):670-7. (Heinisch *et al.,* 2010 a)

Heinisch JJ, Dupres V, Wilk S, Jendretzki A, Dufrêne YF. 2010. Single-molecule

atomic force microscopy reveals clustering of the yeast plasma-membrane sensor Wsc1. PLoS One. 14;5(6):e11104. (Heinisch *et al.,* 2010 b)

Heinisch JJ, Lorberg A, Schmitz HP, Jacoby JJ. 1999. The protein kinase C-mediated MAP kinase pathway involved in the maintenance of cellular integrity in Saccharomyces cerevisiae. Mol Microbiol. May;32(4):671-80.

Hohmann S. 2002. Osmotic stress signaling and osmoadaptation in yeasts. Microbiol Mol Biol Rev. Jun;66(2):300-72.

Inoue H, Nojima H, Okayama H. 1990. High efficiency transformation of Escherichia coli with plasmids. Gene. Nov 30;96(1):23-8.

Kasahara S, Ben Inoue S, Mio T, Yamada T, Nakajima T, Ichishima E, Furuichi Y, Yamada H. 1994. Involvement of cell wall beta-glucan in the action of HM-1 killer toxin. FEBS Lett. Jul 4;348(1):27-32.

Levin DE. 2005. Cell wall integrity signaling in Saccharomyces cerevisiae. Microbiol Mol Biol Rev. 69(2):262-91.

Ponting CP, Hofmann K, Bork P. 1999. A latrophilin/CL-1-like GPS domain in polycystin-1. Curr Biol. Aug 26;9(16):R585-8.

Rajavel M, Philip B, Buehrer BM, Errede B, Levin DE. 1999. Mid2 is a putative sensor for cell integrity signaling in Saccharomyces cerevisiae. Mol Cell Biol. Jun;19(6):3969-76.

Saier MH Jr. 1994. Bacterial sensor kinase/response regulator systems: an introduction. Res Microbiol. Jun-Aug;145(5-6):349-55.

Tatebayashi K, Tanaka K, Yang HY, Yamamoto K, Matsushita Y, Tomida T, Imai M, Saito H. 2007. Transmembrane mucins Hkr1 and Msb2 are putative osmosensors in the SHO1 branch of yeast HOG pathway. EMBO J. 8;26(15):3521-33.

Tang YQ, Han SY, Zheng H, Wu L, Ueda M, Wang XN, Lin Y. 2008. Construction of cell surface-engineered yeasts displaying antigen to detect antibodies by immunofluorescence and yeast-ELISA. Appl Microbiol Biotechnol Jul;79(6):1019-26.

Vay HA, Philip B, Levin DE. 2004. Mutational analysis of the cytoplasmic domain of the Wsc1 cell wall stress sensor. Microbiology. 150(Pt 10) 3281-8

Verna J, Lodder A, Lee K, Vagts A, Ballester R. 1997. A family of genes required for maintenance of cell wall integrity and for the stress response in Saccharomyces cerevisiae. Proc Natl Acad Sci U S A. Dec 9;94(25):13804-9.

Wilk S, Wittland J, Thywissen A, Schmitz HP, Heinisch JJ. 2010. A block of endocytosis of the yeast cell wall integrity sensors Wsc1 and Wsc2 results in reduced fitness in vivo. Sep;284(3):217-29

Wu C, Jansen G, Zhang J, Thomas DY, Whiteway M. 2006. Genes Dev. Adaptor protein Ste50p links the Ste11p MEKK to the HOG pathway through plasma membrane association. Mar 15;20(6):734-46.